TWENTYFIFTH EUROPEAN ROTORCRAFT FORUM

Paper n° G19

Elementary Studies of Active Flap Control with Smart Material Actuators

BY

T.HONGU, M.SATO, E.YAMAKAWA

ADVANCED TECHNOLOGY INSTITUTE OF COMMUTER HELICOPTER

SEPTEMBER 14-16, 1999
R O M E
ITALY

ASSOCIAZIONE INDUSTRIE PER L'AEROSPAZIO, I SISTEMI E LA DIFESA
ASSOCIAZIONE ITALIANA DI AERONAUTICA ED ASTRONAUTICA

Elementary Studies of Active Flap Control with Smart Material Actuators

Tatsuro Hongu, Mitsumasa Sato, and Eiichi Yamakawa

Advanced Technology Institute of Commuter Helicopter, LTD.

Abstract

This paper describes the results of fundamental examination and wind tunnel test of smart material actuators for helicopter rotor system. At the first step, three types of experimental models were made and evaluated. Then, we developed the full scale wind tunnel model with trailing edge active flap which is driven by piezoelectric stack actuation system.

1. Introduction

For rotorcraft, it is very important to suppress the vibration and the noise. Because these vibrations not only affects the ride quality but also causes fatigue damage of the various structural components. And the Blade Vortex Interaction (BVI) noise will be limitation of helicopter operation because it is generated during descent conditions for landing.

In recent years, increasing attention has been devoted to Higher Harmonic Control (HHC) systems which uses swash plate to control the whole blade simultaneously, and Individual Blade Control (IBC) systems which uses individually located actuators to control the each blade. (Refs. 1 to 11)

Since the blade control could be implemented to each individual blade, IBC system can more efficiently suppress the vibration and the noise than HHC concept can. Furthermore IBC can also improve the rotor performance by 2/rev input which HHC can not generate.

ATIC is continuing analytical research about active flap to implement the IBC system(Refs. 12, 13) and smart material actuators to control the active flap on blade. (Ref. 14)

This paper describes the result of a fundamental study and wind tunnel test of such smart material actuators.

2. Fundamental examination

The overview of fundamental examination models are summarized in Table 1. The different two types of Smart Material Actuators are employed for three examination models. One of the actuator is the piezoceramic thin sheets which shaped into parallelogram form and another one is the magnetostrictive actuator.

The first model shown in figure 1 is the aluminum plate twist model which generates the twist deflections of the thin aluminum flat plate by piezoceramic sheets. One end of the plate is fixed to model base and another end is connected to output rod. The piezoceramic sheets are oriented to 45 degrees and directionally bonded to both surface of the aluminum flat plate.

The second model shown in figure 2 is the

X-sectioned composite twist model which generates the twist deflections of graphite-epoxy composite by same way as the aluminum plate twist model. The X-sectioned composite is used to avoid bending deflection loss of the plate and to get large area for piezoceramic sheets.

The third model shown in figure 3 is the hydraulic / mechanical stroke amplifier model which amplifies the stroke output of magnetostrictive actuator. The amplified stroke output of this model is linked to small active flap and the pitch angle of this flap is measured.

The hydraulic amplifier system is consist with a large input piston which is driven by the actuator and a small output bellows. The bellows is used instead of the small piston to minimize the friction and the leakage of oil. Another mechanical amplifier system is consist with long lever and its rotating rod which forms the L-shaped lever. This rod also has the small offset of own axis and the ratio of this offset and lever length is the stroke amplification ratio of this system.

As for the fundamental examinations, static and dynamic tests are conducted. In static condition, the twist deflection of the actuator output rod is measured by rotary encoder. And the moment of output axis is also measured. In dynamic condition, time history of the step response and the frequency response is measured.

3. Results of examination

The results of fundamental examinations are listed in Table 2. In static condition, twist deflection of more than 7 degrees was achieved by the aluminum plate twist model with piezoceramic actuator voltage at 200V. Figure 4 shows the relationship between twist deflection of output rod and actuator input voltage. We can see the hysteresis curve which commonly appears as the characteristics of smart materials. In table 2, the X-sectioned composite twist model shows almost the same twist deflection but doubled output moment against aluminum twist model with the same input voltage. This improvement of output moment is gained by the area increase of the piezoceramic sheets. The relationship between the moment and actuator input voltage for X-sectioned composite twist model is shown in Figure 5. The hysteresis of this figure is smaller than the aluminum twist model.

The result of hydraulic/mechanical stroke amplifier model in table 2 shows the disadvantage in comparison with mechanical

Table 1 Examination Models

Experimental Model	Smart Material Actuator	Stroke amplifier mechanism
Aluminum plate twist	Piezoceramic sheet	Twist the plate by strain of piezo ceramic sheets on both side of plate.
X-sectioned composite twist	Piezoceramic sheet	Use the X-sectioned composite instead of aluminum flat plate to increase piezoceramic sheets.
Hydraulic/mechanical stroke multiplier	Magnetostrictive	Simply multiplies the stroke of actuator by hydraulic piston or mechanical link.

Table 2 Examination results

Examination model	Deflection (degree)	Moment (kgf-mm)
Aluminum plate twist	±7.6	±2.3
X-sectioned composite twist	±7.1	±5.9
Hydraulic stroke multiplier	±3.4	±17.1
Mechanical stroke multiplier	±4.6	±25.8

stroke amplifier system in both deflection and moment output. This result was caused by the friction losses of hydraulic piston. Figure 6 and 7 shows the relationship between the flap deflection and actuator input electric current of hydraulic and mechanical stroke amplifier systems respectively. By the effect of the friction, the hydraulic system has larger hysteresis than mechanical stroke amplifier system.

As the example of result of dynamic response test, Figure 8 shows the time history of the step input response of mechanical stroke amplifier system. We can observe that the response of output twist deflection is very quick, but because of actuator's hysteresis and the friction, output twist deflection does not recover to zero when input current for actuator becomes to zero. As the example of frequency response, bode-plot of X-sectioned composite twist model is shown in Figure 9. Because of resonance with model base, actuator rod or flap model, there is a peak in gain plot at very low frequency (20Hz～30Hz) while the smart material actuator has very high frequency response characteristic.

4. Wind tunnel test

As the next step, we developed the full scale 2-D wind tunnel model to see the feasibility of flap actuation in the realistic environment.

Figure 10 and table 3 shows the overview of the wind tunnel model. The model blade is 1 m span and 0.39m chord with 10%c thick airfoil. And the model has active flap on its trailing edge which is 0.5m span length and 20% chord length.

We selected the piezoceramic stack actuator and mechanical stroke amplifier system which is shown in figure 11 to drive the active flap. And the stroke amplify rate was set to deflect the flap to ±5 degrees.

The actuator was located at 25% chord of the blade and the whole system was equipped inside the blade except the link to flap hinge.

The model has 4 types of sensors which are 3 HALL sensors at flap hinge to measure the flap deflection, LVDT stroke sensor at flap actuation rod to measure the stroke deflection of the rod, strain gauge on flap link to measure the flap hinge moment and stroke sensor of actuator.

The test was conducted with transonic wind tunnel at Kawasaki Heavy Industries,

Table 3 Wind tunnel model

Span	1 m
Chord	0.39 m
Flap span	0.5 m
Flap chord	20 %c
Airfoil section	AK-100D

Ltd. in June 1998. The mach number of this test was 0.3, 0.4, 0.62, and 0.7. And the angle of attack of the blade was varied to 0 and ±4 degrees.

5. Wind tunnel test result

Figure 12 to 15 shows the relationship between the flap hinge moment and the flap deflection of static response test at M=0.3, 0.4, 0.62, and 0.7.

From these figures, we can see that the flap hinge moment became larger as the air speed became higher. At M=0.7, the hinge moment of 90 kgf-mm to -55 kgf-mm was achieved. And the flap deflection which was 2.3 degrees at M=0.3 decreased until 1.1 degrees at M=0.7. And figure 16 shows the difference of the flap deflection by blade angle of attack. There are only small difference between angle of attack 0 and ±4 degrees.

Figure 17 shows the time history of the step input response at M=0.62. From the figure we can see that the LVDT stroke response is very quick.

As the results of frequency response test, figure 18 shows the bode-plot of flap deflection response at M=0.62. It is different from fundamental examination result that the gain plot has no peak because the resonant frequency became higher and the peak has weakened by the damping effect of the air.

From the result of wind tunnel test, we developed the twin actuator system and made the optimization of stroke amplifier ratio.

Figure 19 and 20 shows the schematics of twin actuator systems and concept of there movement. With the figure 19, type 1, both actuators moves in the same direction, and combine there force outputs. Another type, shown in figure 20, actuators moves opposite direction, and there stroke is doubled.

Figure 21 shows the test scene of type 1 model to measure the stiffness of several parts.

With this modification work, we could reach to flap deflection of ±3.2 degrees with 3, 4, 5/rev conditions.

6. Conclusions

In this paper, we described the results of fundamental examination and full scale wind tunnel test of smart material actuators.

By the results of these tests, we could find that the enlargement of actuator power and stiffness of stroke amplifier system is the key term to apply the smart material actuators to the helicopter rotors.

7. References

1 D. Schimke, et al., Individual Blade Control by Servo-Flap and Blade Root Control A Collaborative Research and Development Programme, 23rd ERF, 1997.

2 R. L. Spangler, S. R. Hall, Piezoelectric Actuators for Helicopter Rotor Control, Proc. 31st AIAA Structures, Structual Dynamics, and Materials Conference, 1990.

3 O. Ben-Zeev, I. Chopra, Development of an Improved Helicopter Rotor Model Employing Smart Trailing-Edge Flaps for Vibration Suppression, Proc. SPIE vol. 2443, 1995.

4 M. V. Fulton, R. A. Ormiston, Hover Testing of a Small-Scale Rotor with On-Blade Elevons, 53rd Annual AHS Forum, 1997.

5 F. K. Straub, et al., Application of Smart Materials to Helicopter Rotor Active Control, Proc. SPIE vol. 3044, 1997.

6 R. C. Derham, N. W. Hagood, Rotor Design Using Smart Materials to Actively Twist Blades, 52nd Annual AHS Forum, 1996.

7 F. K. Straub, Active Flap Control for Vibration Reduction and Performance Improvement, 51st Annual AHS Forum, 1995.

8 A. P. F. Bernhard, I. Chopra, Development of

a Smart Moving-Blade-Tip and an Active-Twist Rotor Blade Driven by a Piezo-Induced Bending-Torsion Coupled Beam, 53rd Annual AHS Forum, 1997.

9 S.R.Ghorayeb, et al., Application of Magnetostrictive Smart Materials in Rotor Servoflap Control, Proc. SPIE vol. 2443, 1995.

10 R.Chandra, I.Chopra, Actuation of Trailing Edge Flap in a Wing Model using Piezostack Device, 38th AIAA Structures, Structural Dynamics, and Materials Conference, 1997.

11 T.A.Millott, P.P.Friedmann, The Practical Implementation of an Actively Controlled Flap to Reduce Vibrations in Helicopter Rotors, 49th Annual AHS Forum, 1993.

12 N.Kobiki, et al., Elementary Study for the Effect of HHC and Active Flap on Blade Vortex Interaction, Proc. 23rd ERF Forum, 1997.

13 N.Kobiki, et al., Aeroelastic Analysis and Design for On-blade Active Flap, Proc. 25th ERF Forum, 1999.

14 T.Hongu, et al., Fundamental Study of Smart Material Actuators for Active Flap Control, Proc. AHS International Meeting Heli Japan 98, 1998.

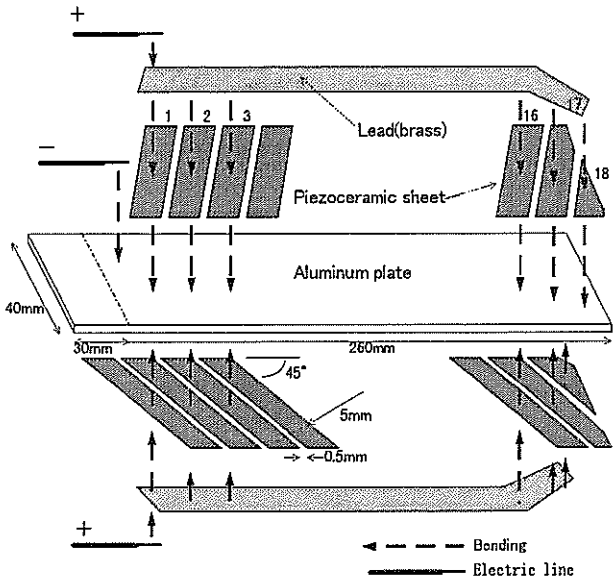

Figure 1 Aluminum plate twist model

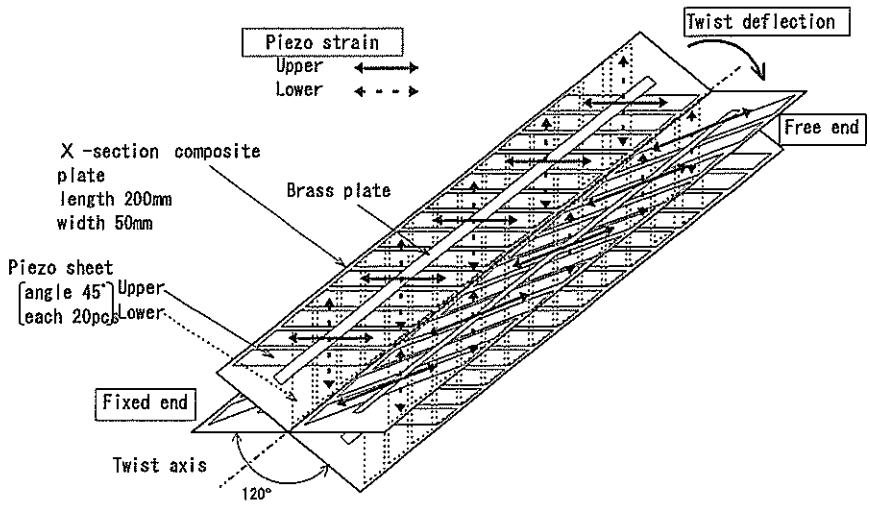

Figure 2 X-sectioned composite twist model

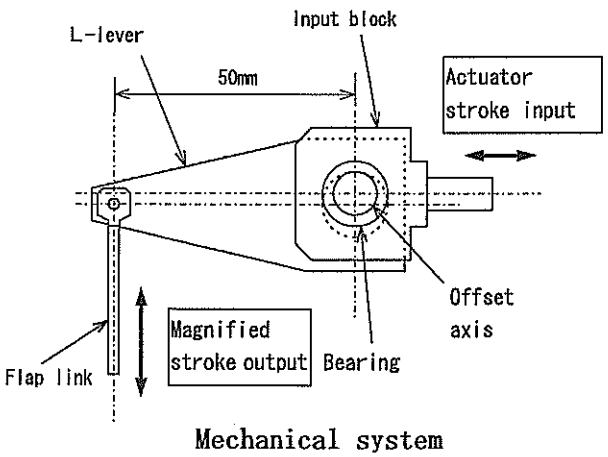

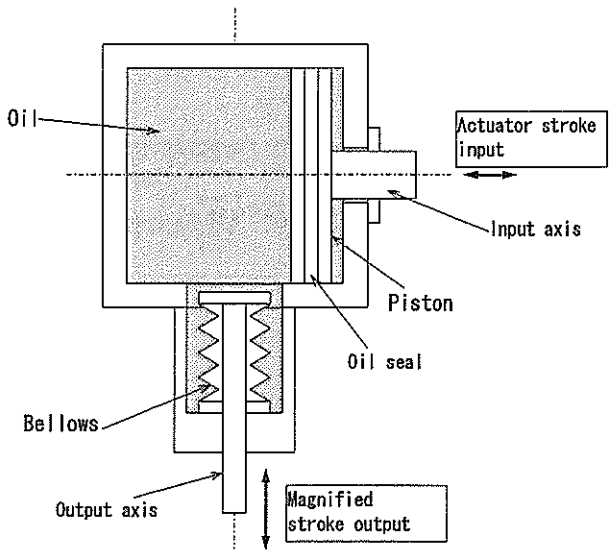

Figure 3 Hydraulic/mechanical stroke multiplier model

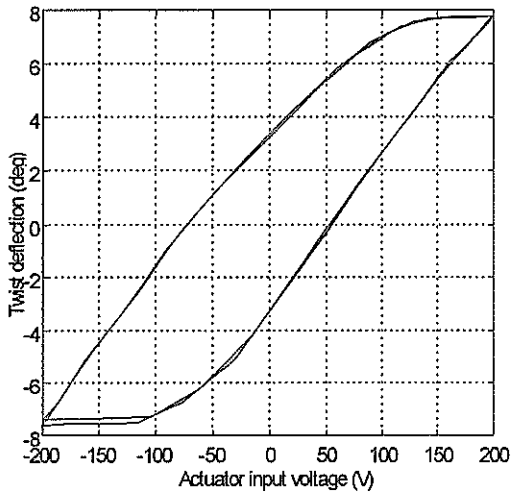

Figure 4 Twist deflection of aluminum twist model

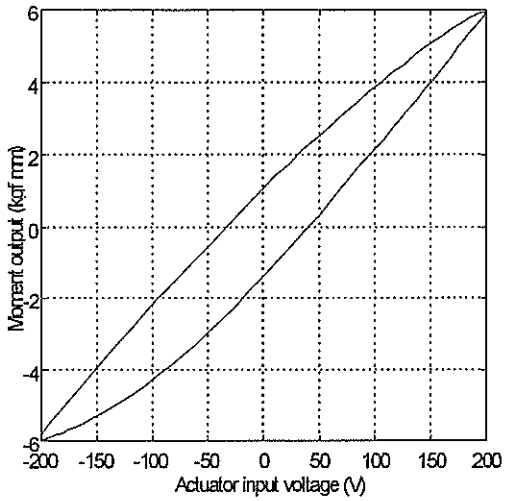

Figure 5 Moment output of composite twist model

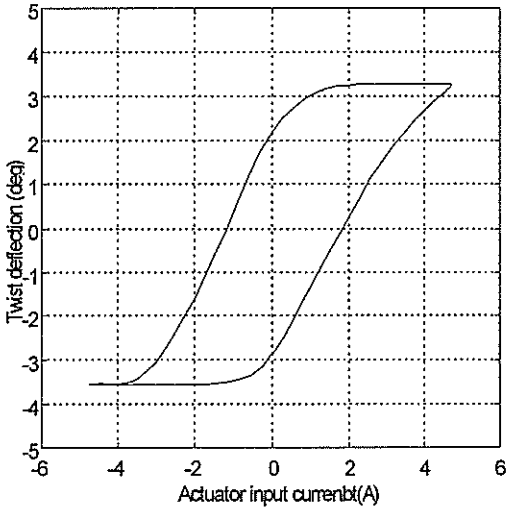

Figure 6 Twist deflection of hydraulic multiply system

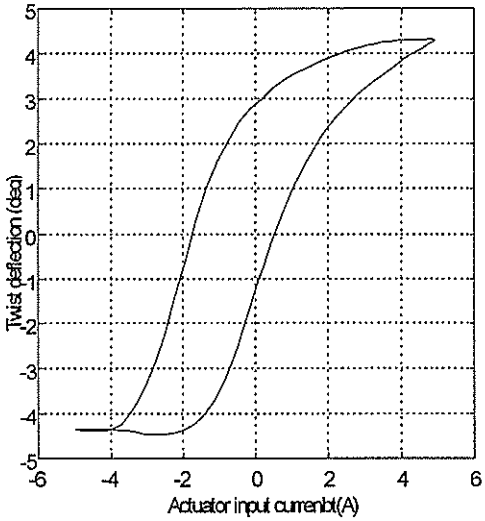

Figure 7 Twist deflection of mechanical multiply system

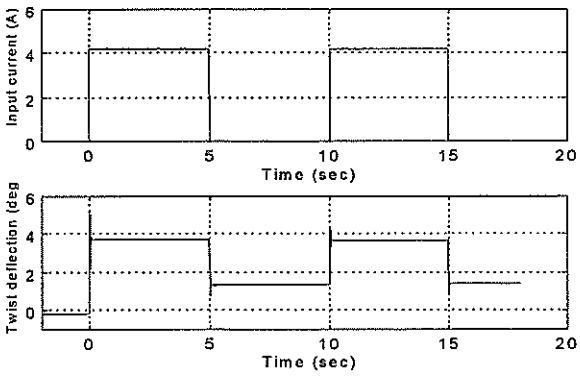

Figure 8 Step response of mechanical multiply system

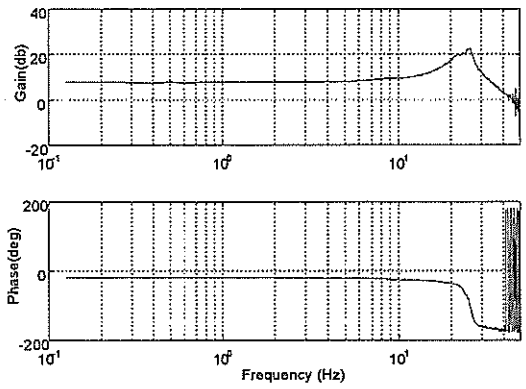

Figure 9 Frequency response of X-sectioned composite twist model

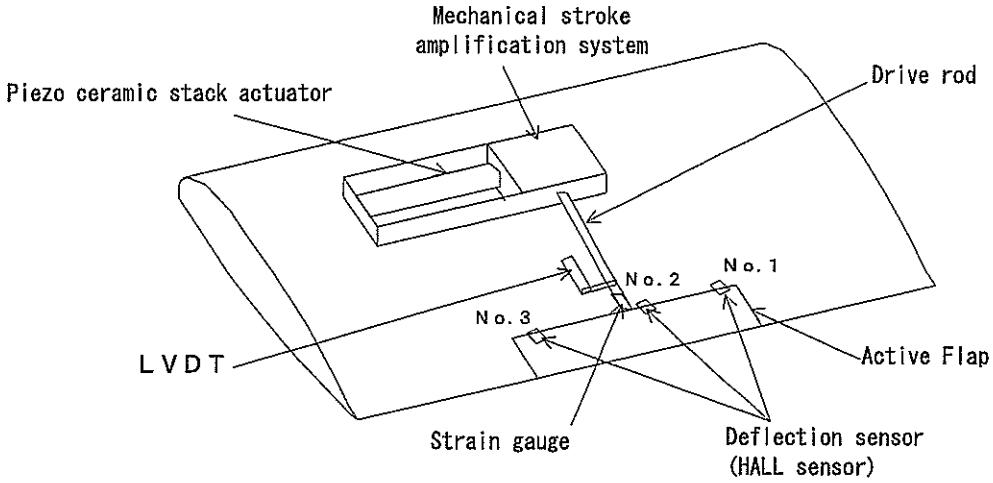

Figure 10 Wind tunnel model

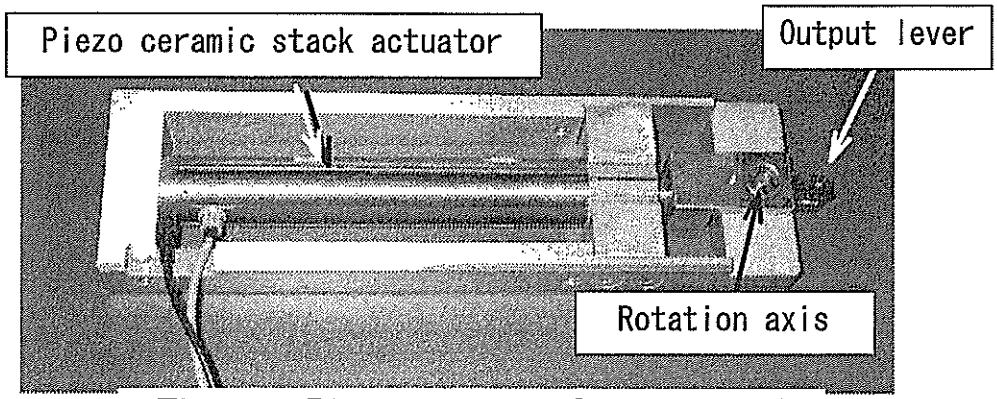

Figure 11 Piezo ceramic stack actuator and stroke amplification mechanism

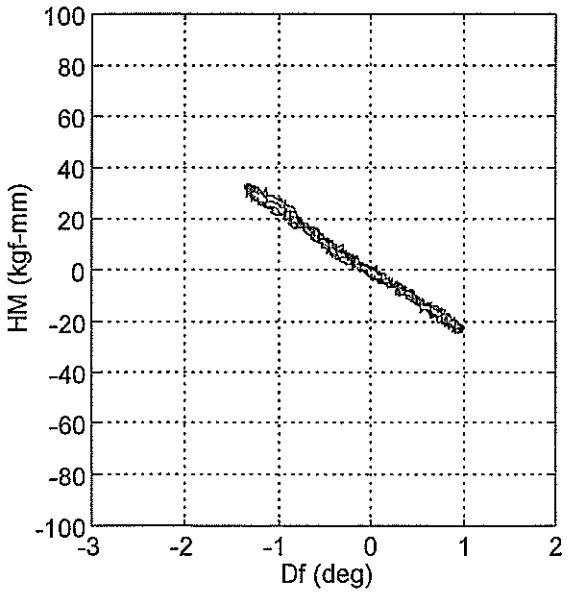

Figure 12 Static response (M=0.3)

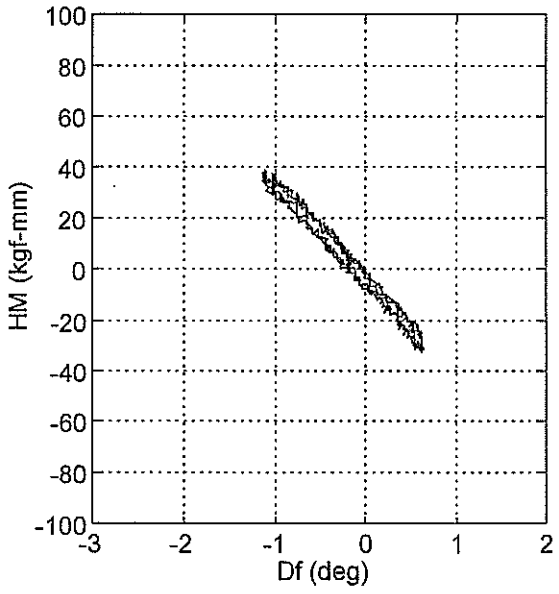

Figure 13 Static response (M=0.4)

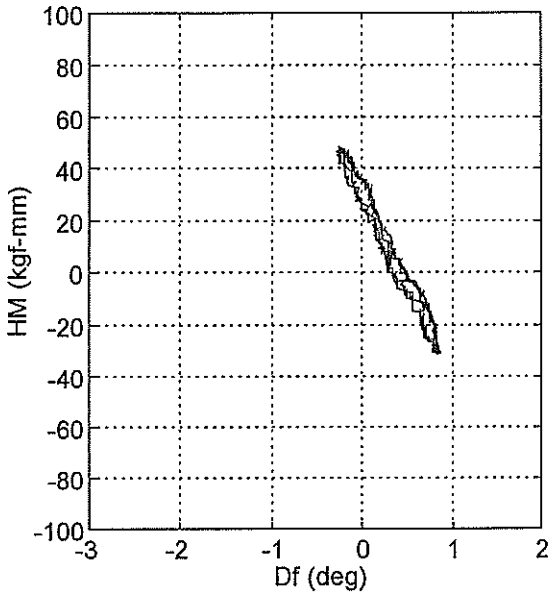

Figure 14 Static response (M=0.62)

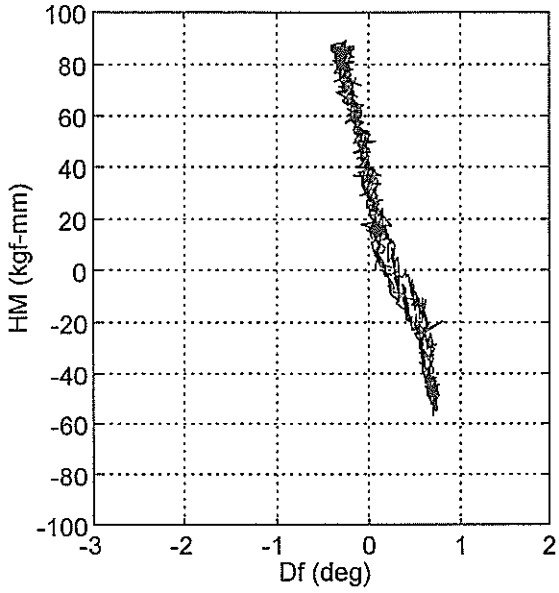

Figure 15 Static response (M=0.7)

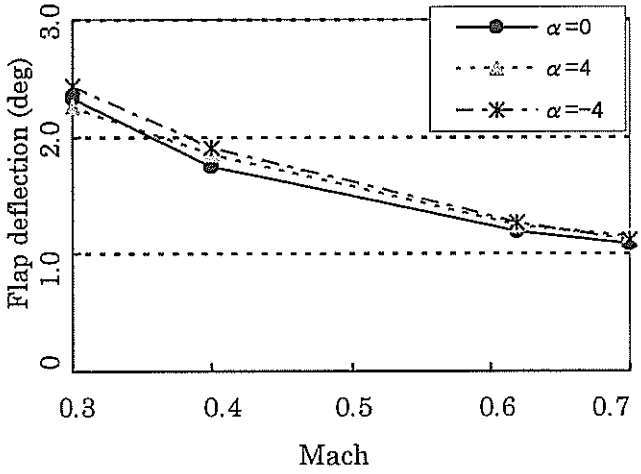

Figure 16 Flap deflection vs. Mach number

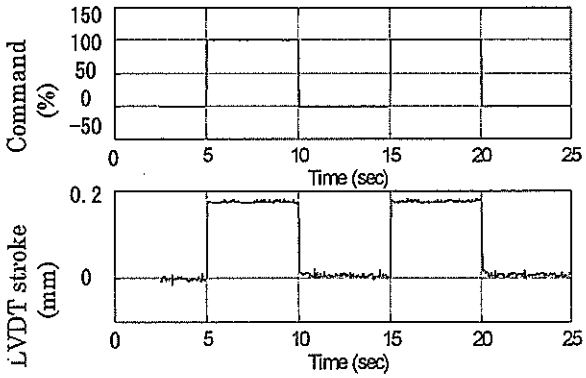

Figure 17 Step response of flap deflection(M=0.62)

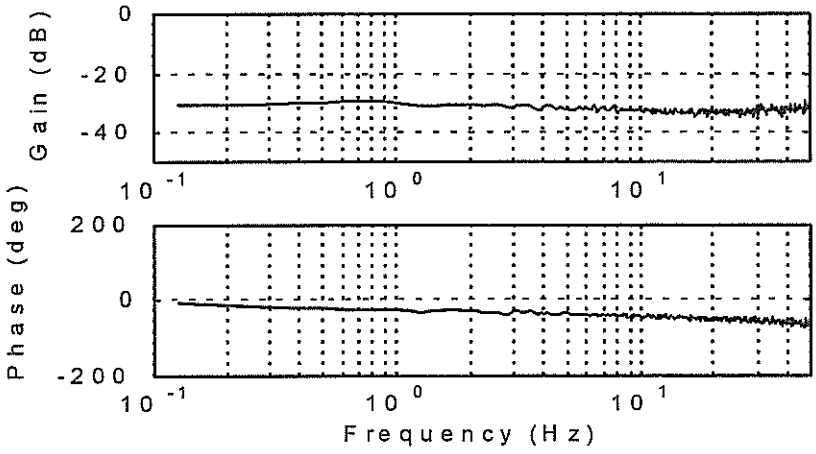

Figure 18 Frequency response of flap deflection(M=0.62)

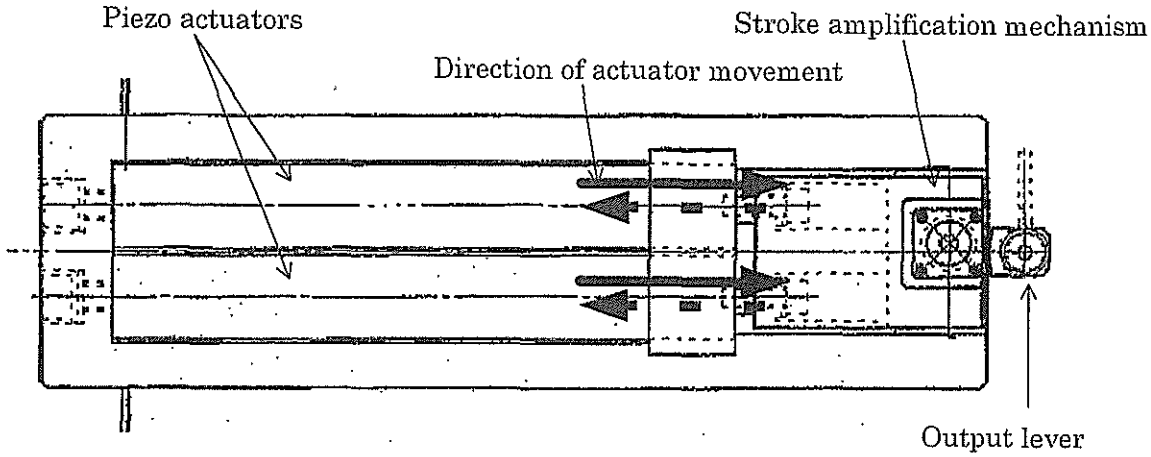

Figure 19 Twin actuation system Type 1

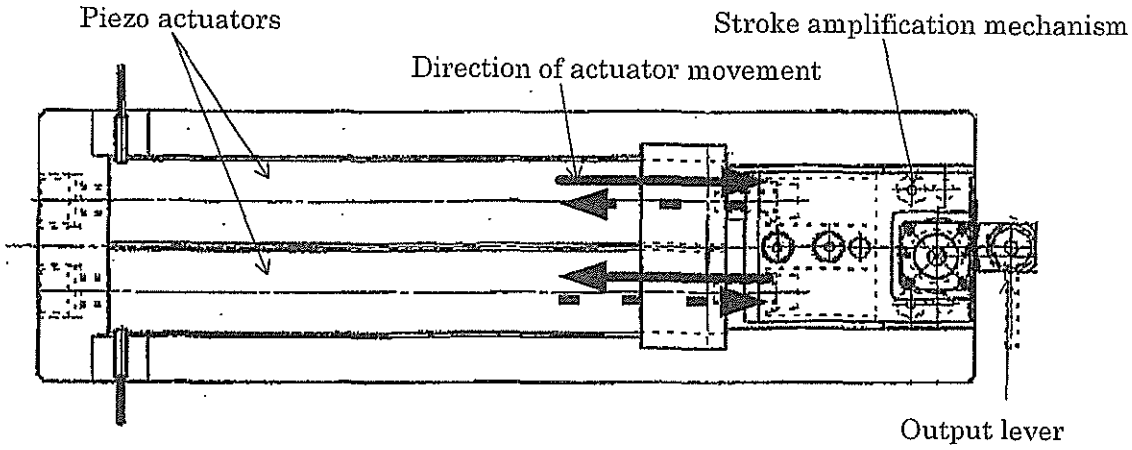

Figure 20 Twin actuation system Type 2

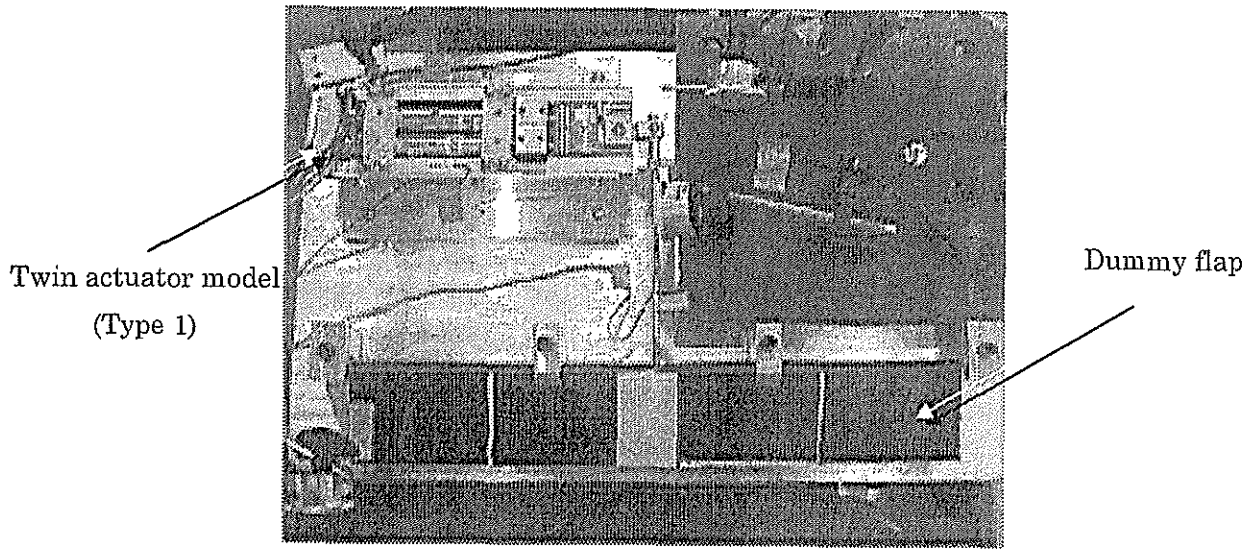

Figure 21 Test scene of type 1 model